Journal of Positive School Psychology http://journalppw.com
2022, Vol. 6, No. 8, 3544-3553

Optimized Video Super Resolution By Predictive Analytics And Machine Learning

Dr. Safinaz S[1] , Dr. K Bhanu Rekha[2]

[1]Assistant Professor -Selection Grade, Presidency University, Electronics and Communication Engineering Dept, Itgalpura Rajanukunte Yelahanka, Bengaluru-560064, Karnataka, India.
[2]Assistant Professor -Selection Grade, Presidency University, Electronics and Communication Engineering Dept, Itgalpura Rajanukunte Yelahanka, Bengaluru-560064, Karnataka, India.

Abstract:

For specific image super-resolution process, HR images are considered by discerning natural image priors and self-similarity enclosed by image and for video super resolution. On the contrary, spatial information through positions and temporal information through frames could be deployed to develop specifics for LR frame. So far numerous research works has been carried out in this region of research and this present research aims to develop an actual hybrid RNN-ACO algorithm for augmenting the video super resolution. To inspect the performance metrics, the research work is carried out in PYTHON tool which displays the accuracy of suggested approach. Deployment of hybrid RNN-ACO model to expand the video super resolution framework will be implemented and the corresponding assessment factors will be analyzed and equated for individual RNN and ACO and collective RNN-ACO model.

Keywords: high resolution, low resolution, Super-resolution.

I. Introduction

Recovery process of high resolution video from its version of low resolution equivalent has gained significant importance and it is stated as super resolution (SR) and applicable in wide areas such as medical imaging, face recognition and satellite imaging. Here, the LR content or files appear in a range of low pass filtered or blurred sate, down sampled and noisy form of the HR data [1]. This kind of undetermined SR issue is especially pronounced for high up-scaling factors in which the texture detail in the restructured SR data are found to be absent.

The optimization factor is predominant which aims at reducing the "mean square error (MSE)" amongst recovered data and the ground truth [2]. In vast majority of the applications, it is quite essential to describe a particular scene model of a high spatial resolution video from an arbitrary input video data. The comparison of a super resolution output to a real world video input makes the difference. Resolution of any image from a video is merely influenced by the acquisition device and so, by increasing the resolution aspect of the acquisition device sensor is unique way to correspondingly increase the resolution of developed image. This method could not be desirable every time because it results in increased price of the device sensor and however the noise content rises while minimizing the size of the pixel.

In other way, one could exploit the fact that even with a LR video camera which runs at "30 frames" per second, one could observe predictions of the equivalent image structure around "30 times" a second [3]. In all these types, the major degradation factor observed was down sampling and compression. Alternatively, "multi-image SR" has been deployed to expand the video for extended period of time. These approaches basically considers an aforementioned distribution of the quantization noise and then integrates the knowledge into "Bayesian SR framework" model or uses the quantization limits to ascertain

convex sets which could oblige the SR problem [13].

In real scenario, the compression artifacts triggered due to the quantization noise are found to be largely reliant on the video content and hectic to be exhibited by means of an open distribution. Performance metrics of the "Bayesian SR" strongly depend on the accuracy of the frame registration and motion assessment and these techniques were not found to be capable of restructuring the high frequency details of the active videos which contains fast and intricate object motions [4]. While the huge motion between the subsequent frames occurs, it becomes a challenging task to locate simultaneous image areas, elusive sub-pixel motion obstinately supports the restoration of details [11] [12]

In [10], a "convolutional neural network" is suggested which is capable to cope up with the variations in illumination, cloud coverage and the landscape features which the general means of challenges presented by fact that dissimilar images are taken over succeeding satellite passages over the identical region of space [9] [10]. This research work focuses on optimization of video super resolution by means of predictive analytics with machine learning models.

II. Literature Review

Two video SR methods tailored for two-stream action recognition were proposed for spatial and temporal streams correspondingly [14] [15]. An effective means of recurrent latent space propagation system is proposed in [16] for fast VSR and the RLSP presents high dimensional underlying conditions to proliferate the temporal means of data among frames in an implied approach. Attained outcomes describe that RLSP is an extremely effectual technique which could compact with VSR issue. A Generative Adversarial Network (GAN) based information is recommended in [17] for VSR problem, termed as VSRResNet along with a novel discriminator architecture to suitable guide VSRResNet during the GAN training. In [18], a simple and robust super resolution based framework is suggested. A novel methodology is proposed [19] for incorporating the temporal way of data in a classified manner where the input sequence is subdivided into various groups, every one relating to a base of frame rate. A deep survey analysis is executed in [20] on recent improvements of image super resolution with the support of deep learning approaches. Current "deep learning" centered "video SP" approaches compensates inter frame motion by means of added frames to the reference one, with support of backward warping. Proper fusion of the image detail from several frames is the vital key to the success of video SR besides motion compensation. Former "CNN" based "video SR systems" could generate sharp edge images where it is not clear that the image details are those intrinsic in input frames or it is learned from the exterior source of data. Moreover, a practical means of property of "SR" systems is the "scalability factor" as in earlier works, the network structure is found to be coupled in a close manner with the SR parameters which makes them less flexible when the new "SR" factors need to be pragmatic [5]. The recent success rate of CNN is attained based on a deep neural networks emerged with the promising performance metrics. Training of the CNNs could be accomplished in an efficient manner by parallelization using GPU-accelerated computing. In classification and retrieval, the CNNs have been productively trained on video data, but the training phase is tedious task as the video quality provisions for the training database are found to be high since the CNN output is the actual video rather than a label. Appropriate videos for SR tasks are uncompressed, feature rich and it should be separated by means of scenes or shots and by pre-training the CNN with images, the creation of a huge video database could be avoided [6].

At the instant of adopting a method from the images to videos, it is generally advantageous to deploy the basic knowledge that the frames of the same scene of a video could be approximated

by a mere image and a motion configuration. Hence, predicting and compensating the motion features is the most powerful mechanism to further constrain the issue and expose temporal based correspondences [7]. In [8], a novel method of "video super resolution", termed as "Recurrent Back-Projection Network (RBPN)" is suggested in which the spatial and temporal backgrounds from continuous video frames were integrated by means of a "recurrent encoder-decoder module".

III. Proposed Methodology

In this research, the video super resolution is carried out by hybrid RNN-ACO model which would support video enhancement by collecting all relevant information from the video patches. For example, when a video is captured in a camera and normal mobile phone, the resolution of camera video would be clearer when compared to other one. This hybrid model (RNN-ACO) helps to retrieve all possible information from the actual video. The steps included in this research are given as follows:

Step 1: Initially, the video is converted to image format.

Step 2: Patch extraction phase is carried out and here, every patch is detached from pixels value and they are organized depending on its energy and high level of energy retained by thresholding. Then the patches are restructured in column to from pattern.

Step 3: Once patch extraction is done, the analysis takes place by means of mapping. Here, the linear and non-linear state is identified. Vectors are formed to identify non-linear state.

Step 4: Then reconstruction occurs. During reconstruction, all relevant information may not be present. Some of the essential features may be lost and so, hybrid RNN-ACO model is deployed.

Step 5: Recurrent Neural Networks-Ant Colony Optimization

For any continuous means of system, genetic way of regulation model could be symbolized with the support of recurrent neural network based formulation,

$$\tau_i \frac{de_i}{dt} = f\left(\sum_{j=1}^{N} w_{ij} e_j + \sum_{j=1}^{N} v_{ik} u_k + \beta_i\right) - \lambda_i e_i \quad (1)$$

Where,

e_i is gene expression level for i^{th} gene, f() is a nonlinear function

This model could moreover be categorized in a discrete form:

$$\frac{e_i(t+\Delta t) - e_i(t)}{\Delta t} = \frac{1}{\tau_i}\left(f\sum_{j=1}^{N} w_{ij} e_j(t) + \sum_{k=1}^{K} v_{ik} u_k(t) - \beta_i) - \lambda_i e_i(t)\right), or,$$

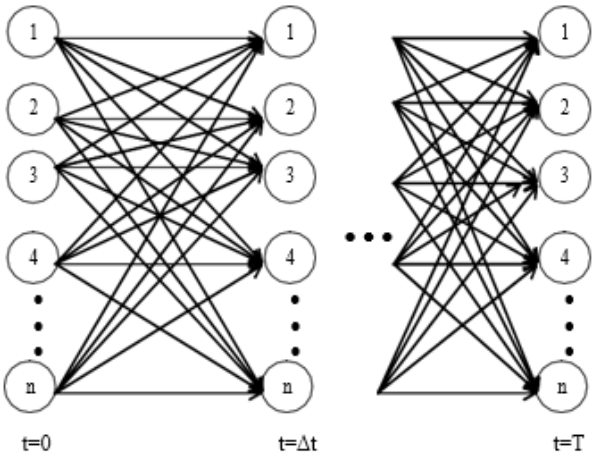

Figure 1. Portrayal of genetic network over RNN

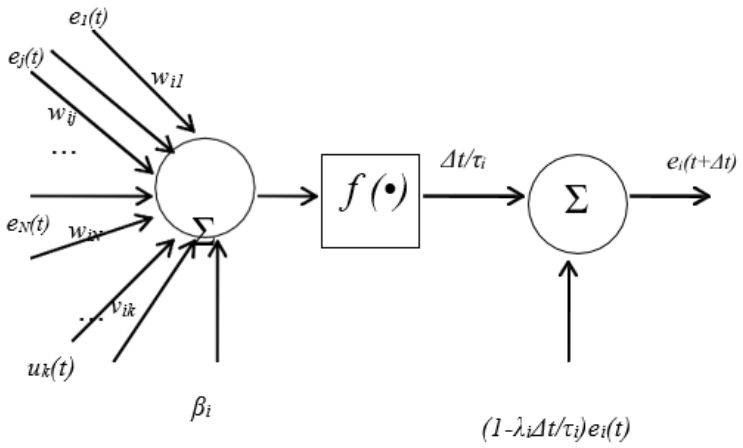

Figure 2. Single node in RNN model

$$e_i(t+\Delta t)=\frac{\Delta t}{\tau_i} f\left(\sum_{j=1}^{N} w_{ij} e_j(t)+\sum_{k=1}^{K} v_{ik} u_k(t)+\beta_i\right)+\left(1-\frac{\lambda_i \Delta t}{\tau_i}\right) e_i(t)$$

(2)

Figure 1 represents RNN, which is extended in time from t=0 to T with an interval Δt, for forming a genetic network. At this point, every node resembles to a gene, and a link amongst 2 nodes describes their interface. The weight values could be either positive, negative, or zero, as stated directly above. Figure 2 demonstrates a node in the recurrent neural network, which apprehends equation 2.

It is normally challenging to accomplish depths of external variables, so it is a communal practice to ignore $\sum_{k} v_{ik} u_k(t)$. Though this interpretation inexorably disturbs the accuracy of models, studies based on it still offer several stimulating intuitions into gene networks, as established. From the subsequent section, it could be seen that presence of these exogenous inputs does not affect derivation of learning system. For computational easiness, it is moreover presumed that decay rate parameter λ is 1. The final model processed in research is signified as

$$e_i(t+\Delta t)=\frac{\Delta t}{\tau_i}\times f\left(\sum_{j=1}^{N} w_{ij} e_j(t)+\beta_i\right)+\left(1-\frac{\Delta t}{\tau_i}\right) e_i(t)$$

(3)

Even though the model has formerly been stated, the exertion of RNN training confines its additional application for gene network implication. Here, this research intends to combine ant colony optimization to use a diverse training approach, and to define indefinite network considerations.

In this methodology, the sub-pixel optimization is achieved by ACOR process.

As a distinctive creation of combinatorial problems, continuous optimization is determined by a search-space S considered to control above a set of decision variables and an objective function f: S R R0 1 to be reduced. S is a set of continuous variables Xi, i 5 1,…. n, and it has the controlled or unrestrained variables, i.e., vi g D domain. A solution s* g S is the best pattern of continuous variables and it is measured as an inclusive optimal solution if and only if f(s*) d f(s) for all possible f(s) g S. The set of all inclusive optimal solutions is offered by S* # S, where at least one s* should be found to resolve the constant optimization problem.

Two penalizer terms were used in cost-function: a data term and a sharpness measure.

Consider a candidate solution comprising LR images transmuted by a matrix-matching, connected with a HR image I. The energy E of this solution is termed as:

$$E(I,L)=\alpha\sum_{i=1}^{m}(L_i-I)^2+\beta(\nabla I)$$

Where L is set of transformed LR observations, and m is cardinality of L. Above-mentioned equation is analogous to the overall design for super-resolution. As the LR set is obtained upon spatial displacements, certain diffraction patterns might vary conferring to the position of the light-source, shape and height of object-plane, and holographic fringes might be marginally changed for all LR image.

Step 6: Then, the vectors gets multiplied and new image is formed. Now, the newly formed image is compared with the actual image and the comparative resolution pattern is achieved.

IV. Results

This section describes the results attained from the proposed research method. When the video gets spread, the weight distribution of video changes during each iteration process. Based on the data available, the geometric analysis of the pattern is given in Figure 3.

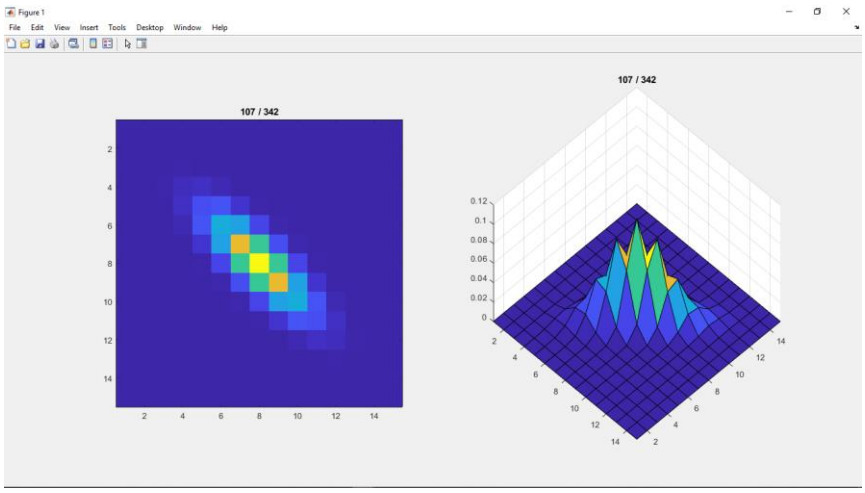

Figure 3: Geometric analysis

As the resolution increases, the video super resolution gets improved to an extent. Resolutino pattern of the video is described in Figure 4.

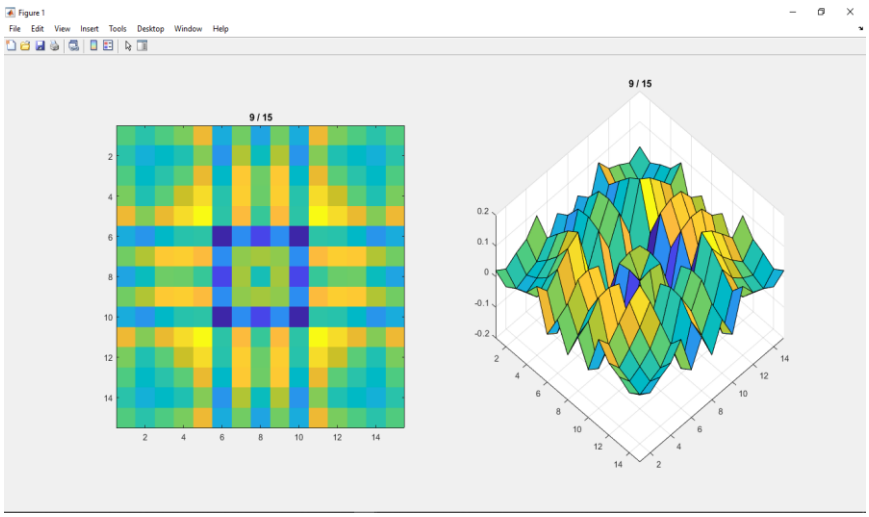

Figure 4: Resolution analysis

The comparative resolution pattern of actual video image ans the newly formed one is given in Figure 5 and 6.

225x225 double

1	2	3	4	5	6	7	8	9	10	11	12
7.4787e-06	1.5026e-05	2.3882e-05	3.5344e-05	4.7617e-05	5.7645e-05	6.2657e-05	6.1061e-05	5.3287e-05	4.1629e-05	2.9132e-05	1.8286e-05
1.5026e-05	3.5042e-05	5.7189e-05	8.4786e-05	1.1302e-04	1.3540e-04	1.4599e-04	1.4124e-04	1.2235e-04	9.4809e-05	6.5762e-05	4.0891e-05
2.3882e-05	5.7189e-05	1.1378e-04	1.8390e-04	2.4499e-04	2.8993e-04	3.0954e-04	2.9665e-04	2.5461e-04	1.9545e-04	1.3422e-04	8.2602e-05
3.5344e-05	8.4786e-05	1.8390e-04	3.3943e-04	4.8421e-04	5.6699e-04	5.9870e-04	5.6634e-04	4.8005e-04	3.6428e-04	2.4737e-04	1.5053e-04
4.7617e-05	1.1302e-04	2.4499e-04	4.8421e-04	8.1450e-04	0.0010	0.0011	9.8316e-04	8.1896e-04	6.1252e-04	4.1078e-04	2.4701e-04
5.7645e-05	1.3540e-04	2.8993e-04	5.6699e-04	0.0010	0.0016	0.0017	0.0016	0.0013	9.2688e-04	6.1308e-04	3.6425e-04
6.2657e-05	1.4599e-04	3.0954e-04	5.9870e-04	0.0011	0.0017	0.0024	0.0022	0.0018	0.0013	8.2142e-04	4.8194e-04
6.1061e-05	1.4124e-04	2.9665e-04	5.6634e-04	9.8316e-04	0.0016	0.0022	0.0027	0.0022	0.0016	9.8916e-04	5.7153e-04
5.3287e-05	1.2235e-04	2.5461e-04	4.8005e-04	8.1896e-04	0.0013	0.0018	0.0022	0.0023	0.0017	0.0011	6.0519e-04
4.1629e-05	9.4809e-05	1.9545e-04	3.6428e-04	6.1252e-04	9.2688e-04	0.0013	0.0016	0.0017	0.0016	0.0010	5.6739e-04
2.9132e-05	6.5762e-05	1.3422e-04	2.4737e-04	4.1078e-04	6.1308e-04	8.2142e-04	9.8916e-04	0.0011	0.0010	7.9593e-04	4.6534e-04
1.8286e-05	4.0891e-05	8.2602e-05	1.5053e-04	2.4701e-04	3.6425e-04	4.8194e-04	5.7153e-04	6.0519e-04	5.6739e-04	4.6534e-04	3.2082e-04
1.0312e-05	2.2839e-05	4.5658e-05	8.2279e-05	1.3346e-04	1.9452e-04	2.5441e-04	2.9814e-04	3.1207e-04	2.9029e-04	2.3997e-04	1.7759e-04
5.2348e-06	1.1482e-05	2.2721e-05	4.0508e-05	6.4980e-05	9.3663e-05	1.2116e-04	1.4045e-04	1.4560e-04	1.3461e-04	1.1113e-04	8.2044e-05
2.3957e-06	5.2060e-06	1.0202e-05	1.8005e-05	2.8588e-05	4.0787e-05	5.2230e-05	5.9964e-05	6.1629e-05	5.6612e-05	4.6499e-05	3.4257e-05
1.4625e-05	2.7654e-05	4.6296e-05	7.0618e-05	9.7017e-05	1.1943e-04	1.3159e-04	1.2959e-04	1.1399e-04	8.9562e-05	6.2918e-05	3.9586e-05

Figure 5: Actual image resolution table

15x10000 double

1	2	3	4	5	6	7	8	9	10	11	12	13	14	15	16	17
-3.6968e-04	-0.0060	-8.8408e-04	-1.7655e-05	5.3352e-04	-0.0019	-1.4809e-04	-2.9191e-05	-0.0076	0.0022	0.0016	-0.0030	3.9681e-04	3.2665e-04	4.2790e-04	1.9083e-04	9.3462e-04
0.0024	-0.0157	-0.0103	0.0040	-6.0533e-04	0.0012	-0.0038	2.8311e-04	0.0049	0.0039	-0.0049	-0.0127	0.0023	-0.0028	0.0027	5.8894e-04	0.0066
-5.5303e-04	-0.0027	-0.0028	0.0044	-4.6049e-04	-1.1255e-04	-0.0014	-0.0011	-0.0034	0.0059	-0.0052	-0.0028	0.0012	0.0024	-9.3656e-04	0.0026	-0.0029
-0.0042	0.0122	0.0055	0.0046	0.0059	4.0543e-04	0.0023	-0.0066	-0.0107	0.0221	-0.0052	-0.0079	0.0042	-0.0055	0.0023	9.7300e-04	0.0056
2.9642e-04	-0.0014	9.0334e-06	9.6396e-04	-5.4450e-04	-1.7988e-04	-2.4342e-05	4.2677e-04	0.0350	-0.0043	0.0018	0.0033	-4.8341e-04	0.0011	-5.0422e-04	1.2159e-05	-0.0010
0.0166	0.0030	-0.0105	-0.0031	-0.0146	-0.0277	-0.0082	0.0080	-0.0094	5.2097e-04	-0.0023	-0.0233	-0.0119	0.0062	-0.0096	-0.0067	-0.0024
-6.6733e-04	-0.0069	0.0023	-0.0047	0.0033	0.0068	0.0019	-0.0012	0.0599	3.4385e-04	-0.0031	0.0046	0.0025	9.0908e-04	0.0025	0.0011	0.0056
-0.0065	0.0105	0.0026	-0.0093	5.1172e-04	-0.0052	0.0023	0.0094	-0.0186	0.0488	0.0218	-0.0068	-0.0026	-0.0169	0.0043	-0.0084	0.0078
-0.0150	-0.0381	-0.0115	-0.0043	4.8063e-04	-0.0023	-0.0043	-8.5482e-06	-0.0226	-0.0174	-0.0125	0.0456	0.0038	-0.0089	0.0040	0.0019	-0.0024
0.0065	-0.0132	-0.0102	0.0144	-0.0099	-0.0220	-0.0076	0.0038	0.0238	0.0372	-3.5841e-04	-0.0264	-0.0084	0.0012	-0.0070	-0.0061	0.0087
0.0145	-0.0089	-3.2805e-04	-0.0499	9.6586e-04	-0.0111	-5.0961e-04	-0.0119	0.1041	0.0697	-0.0227	-0.0086	0.0031	0.0217	-0.0023	0.0081	0.0346
0.0116	-0.0095	-0.0341	0.0604	-0.0387	0.0581	-0.0355	-0.0197	0.0176	-0.0324	-0.0222	0.0649	-0.0389	-0.0173	-0.0381	-0.0360	0.0711
0.0133	0.0410	0.0247	-0.0076	0.0190	-0.0348	0.0207	0.0100	0.0451	-0.0127	0.0226	0.0502	0.0168	0.0154	0.0164	0.0161	-0.0093
-0.1010	-0.0809	-0.0713	-0.0737	-0.0667	0.0717	-0.0763	-0.0959	-0.0592	0.2107	-0.0862	0.1476	-0.0711	-0.0933	-0.0748	-0.0786	-0.0670
-0.1605	-0.0999	-0.0694	-0.2567	-0.0619	-0.4319	-0.0762	-0.1202	-0.1693	-0.5345	-0.1012	-0.4966	-0.0683	-0.1167	-0.0738	-0.0803	-0.2717

Figure 6: Newly formed image resolution table

Figure 7: Enhancement of image dimensions

Figure 7 denotes the enhancement of image dimensions and in Figure 8, the blue line represents the proposed approach with hybrid RNN-ACO output accuracy and yellow line denoted the conventional output without hybrid model.

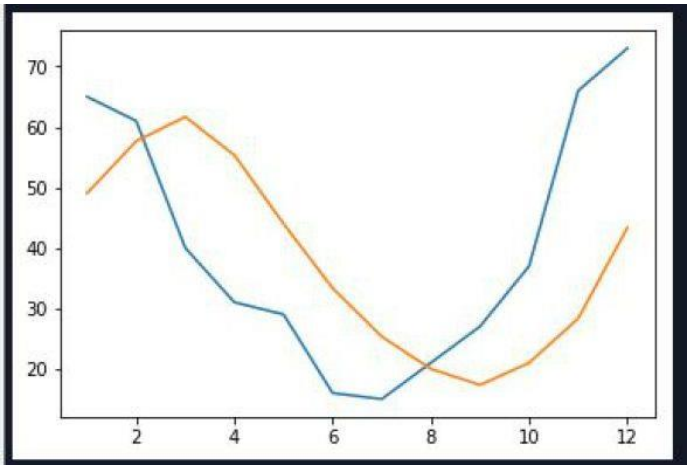

Figure 8: Accuracy improvement in actual versus predicted

Similarly, the resolution graph for proposed and actual image is given in Figure 9, which shows that proposed resolution is better (blue graph) than old one (yellow graph).

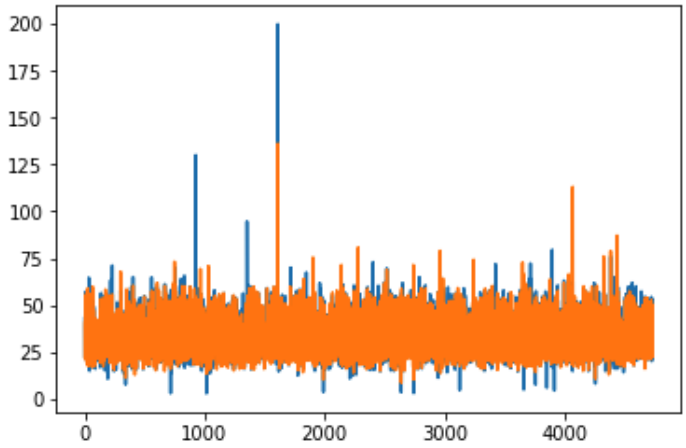

Figure 9: Actual versus resolution enhancement

Comparative table which shows the performance metrics of conventional methods and the hybrid approach.

Table 1: Comparative table

Parameter	RF	ACO	RNN+ACO
Precision	0.72	0.71	0.83
Recall	0.81	0.92	0.87
Fscore	0.76	0.80	0.849

Accuracy	0.72	0.68	0.83
Resolution level	3rd level	6th level	8th level
SSIM	0.5	0.62	0.73
IFC	50%	65%	71%
VII	62%	58%	69%
FII	38%	27%	52%

V. Conclusion

This research focused on video super resolution by means of hybrid RNN-ACO model. Here, the quality of images and its reconstruction phase is enhanced without losing any relevant form of information by the hybrid approach. The research was carried out in python environment and efficacy of the model is analyzed with the means of performance evaluation metrics. The comparison table (Table 1) shows the efficiency of the proposed method.

Statements & Declarations

Funding

Authors declare that there was no such funds, grants or other support were received during the preparation of this manuscript.

Declaration

We, author(s) of the above titled research paper hereby declare that the work encompassed in the above paper is unique and is a conclusion of the research carried out by the authors specified in it.

Competing Interests

Authors have no significant financial or non-financial interests to disclose.

Author Contributions

All authors contributed to this research work including data analysis, literature survey. The initial draft was prepared by Dr. Safinaz and reviewed by Dr. Bhanu Rekha. Both of the authors read and approved the final draft.

Data Availability

Datasets created during the analysis of current research are available from first author on reasonable request.

References

[1] Shi, W., Caballero, J., Huszár, F., Totz, J., Aitken, A. P., Bishop, R., ... & Wang, Z. (2016). Real-time single image and video super-resolution using an efficient sub-pixel convolutional neural network. In Proceedings of the IEEE conference on computer vision and pattern recognition (pp. 1874-1883).

[2] Ledig, C., Theis, L., Huszár, F., Caballero, J., Cunningham, A., Acosta, A., ... & Shi, W. (2017). Photo-realistic single image super-resolution using a generative adversarial network. In Proceedings of the IEEE conference on computer vision and pattern recognition (pp. 4681-4690).

[3] Mitzel, D., Pock, T., Schoenemann, T., & Cremers, D. (2009, September). Video super resolution using duality based tv-l 1 optical flow. In Joint Pattern Recognition Symposium (pp. 432-441). Springer, Berlin, Heidelberg.

[4] Xiong, Z., Sun, X., & Wu, F. (2010). Robust web image/video super-resolution. IEEE transactions on image processing, 19(8), 2017-2028.

[5] Tao, X., Gao, H., Liao, R., Wang, J., & Jia, J. (2017). Detail-revealing deep video super-resolution. In Proceedings of the IEEE International Conference on Computer Vision (pp. 4472-4480).

[6] Kappeler, A., Yoo, S., Dai, Q., & Katsaggelos, A. K. (2016). Video super-resolution with convolutional neural networks. IEEE transactions on computational imaging, 2(2), 109-122.

[7] Caballero, J., Ledig, C., Aitken, A., Acosta, A., Totz, J., Wang, Z., & Shi, W. (2017). Real-time video super-resolution with spatio-temporal networks and motion compensation. In Proceedings of the IEEE Conference on Computer Vision and Pattern Recognition (pp. 4778-4787).

[8] Haris, M., Shakhnarovich, G., & Ukita, N. (2019). Recurrent back-projection network for video super-resolution. In Proceedings of the IEEE/CVF Conference on Computer Vision and Pattern Recognition (pp. 3897-3906).

[9] Li, S., He, F., Du, B., Zhang, L., Xu, Y., & Tao, D. (2019). Fast spatio-temporal residual network for video super-resolution. In Proceedings of the IEEE/CVF Conference on Computer Vision and Pattern Recognition (pp. 10522-10531).

[10] Märtens, M., Izzo, D., Krzic, A., & Cox, D. (2019). Super-resolution of PROBA-V images using convolutional neural networks. Astrodynamics, 3(4), 387-402.

[11] Xiang, X., Tian, Y., Zhang, Y., Fu, Y., Allebach, J. P., & Xu, C. (2020). Zooming slow-mo: Fast and accurate one-stage space-time video super-resolution. In Proceedings of the IEEE/CVF conference on computer vision and pattern recognition (pp. 3370-3379).

[12] Wang, L., Guo, Y., Liu, L., Lin, Z., Deng, X., & An, W. (2020). Deep video super-resolution using HR optical flow estimation. IEEE Transactions on Image Processing, 29, 4323-4336.

[13] Yi, P., Wang, Z., Jiang, K., Jiang, J., & Ma, J. (2019). Progressive fusion video super-resolution network via exploiting non-local spatio-temporal correlations. In Proceedings of the IEEE/CVF International Conference on Computer Vision (pp. 3106-3115).

[14] Zhang, H., Liu, D., & Xiong, Z. (2019). Two-stream action recognition-oriented video super-resolution. In Proceedings of the IEEE/CVF International Conference on Computer Vision (pp. 8799-8808).

[15] Tian, Y., Zhang, Y., Fu, Y., & Xu, C. (2020). Tdan: Temporally-deformable alignment network for video super-resolution. In Proceedings of the IEEE/CVF Conference on Computer Vision and Pattern Recognition (pp. 3360-3369).

[16] Fuoli, D., Gu, S., & Timofte, R. (2019, October). Efficient video super-resolution through recurrent latent space propagation. In 2019 IEEE/CVF International Conference on Computer Vision Workshop (ICCVW) (pp. 3476-3485). IEEE.

[17] Lucas, A., Lopez-Tapia, S., Molina, R., & Katsaggelos, A. K. (2019). Generative adversarial networks and perceptual losses for video super-resolution. IEEE Transactions on Image Processing, 28(7), 3312-3327.

[18] Brifman, A., Romano, Y., & Elad, M. (2019). Unified single-image and video super-resolution via denoising algorithms. IEEE Transactions on Image Processing, 28(12), 6063-6076.

[19] Isobe, T., Li, S., Jia, X., Yuan, S., Slabaugh, G., Xu, C., ... & Tian, Q. (2020). Video super-resolution with temporal

group attention. In Proceedings of the IEEE/CVF Conference on Computer Vision and Pattern Recognition (pp. 8008-8017).

[20] Wang, Z., Chen, J., & Hoi, S. C. (2020). Deep learning for image super-resolution: A survey. IEEE transactions on pattern analysis and machine intelligence, 43(10), 3365-3387.